Optical nucleon-deuteron potential

J. Kuroś,[1] H. Witała,[1] W. Glöckle,[2] J. Golak,[1] D. Hüber,[2] and H. Kamada[2]
[1]*Institute of Physics, Jagellonian University, PL-30059 Cracow, Poland*
[2]*Institut für Theoretische Physik II, Ruhr-Universität Bochum, D-44780 Bochum, Germany*
(Received 21 February 1997)

Nucleon-deuteron scattering is cast into the form of an optical potential formalism. Two forms of an optical potential are given. The resulting integral equations for the optical potentials are approximated by the first two leading terms. Our numerical results demonstrate that even at intermediate energies these approximations are insufficient to cover all of the angular range. Rescattering terms of higher order in the nucleon-nucleon (NN) t matrix are needed. If one focuses on forward scattering, low-order approximations in the NN t matrix can be sufficient, depending on energy, and observable. [S0556-2813(97)00608-0]

PACS number(s): 21.45.+v, 24.10.Ht, 25.10.+s

I. INTRODUCTION

In recent years it has become possible to numerically solve the three nucleon Faddeev equations with high precision using any realistic nucleon-nucleon (NN) force and even adding three-nucleon forces [1–4]. Therefore this system appears to be a promising candidate to rigorously study properties of optical potentials which describe the effective interaction between the nucleon and the deuteron.

Optical potentials have a long tradition [5–9]. However, their theoretical derivation from the underlying N-particle Hamiltonian poses a serious problem and actual realizations have been carried through at intermediate energies in the spectator expansion scheme [7–9] and at lower energies in the framework of dispersion relations [10]. At intermediate energies the resulting expressions have the typical ''$t\rho$'' form, where t is a NN t matrix and ρ the single particle density matrix of the target. That form is the leading term in an expansion in the NN t matrix. Whether this truncation is justified from a theoretical point of view is difficult to assess because of the underlying many-body problem. In a few-nucleon system, however, one may hope to get quantitative insight into the way the optical potential builds up by rescattering processes of increasing order. This has been formulated recently in the context of the Faddeev-Yakubowsky scheme for very light nuclei [11]. In the present article we restrict ourselves to the deuteron target and carry out numerical studies.

In Sec. II we present the formalism for casting nucleon-deuteron (n-d) scattering into the form of an optical potential scattering problem. Our numerical study is shown in Sec. III. We conclude in Sec. IV.

II. THE *n*-*d* OPTICAL POTENTIAL

We start from the operator U for elastic n-d scattering which obeys the Alt-Grassberger-Sandhas (AGS) equations [12,13]

$$U = PG_0^{-1} + PtG_0U. \tag{1}$$

Here t is the off-shell nucleon-nucleon t matrix generated through the Lippmann-Schwinger equation from the particular NN interaction V, P is the sum of a cyclic and an anticyclic permutation of three nucleons, and G_0 the free three-nucleon propagator. We work in the isospin formalism and treat the nucleons as identical. The operators in Eq. (1) are to be applied onto the initial channel state

$$|\phi_{\vec{q}_0}\rangle \equiv |\varphi_d\rangle|\vec{q}_0\rangle \tag{2}$$

built from the deuteron wave function $|\varphi_d\rangle$ and the momentum eigenstate of relative motion $|\vec{q}_0\rangle$ of the incoming nucleon with respect to the deuteron.

One can decompose tG_0 in Eq. (1) into two parts. In the first one the two nucleons propagate as a deuteron and in the second they are in two-body scattering states:

$$tG_0 = V\frac{1}{E-H_0-V+i\varepsilon} = VG_d + VG_c, \tag{3}$$

with

$$G_d \equiv |\varphi_d\rangle \frac{1}{E-(3/4m)q^2-E_d+i\varepsilon}\langle\varphi_d|, \tag{4}$$

$$G_c \equiv \int d\vec{p}\,|\varphi_{\vec{p}}\rangle^{(+)}\frac{1}{E-(3/4m)q^2-(1/m)p^2+i\varepsilon}{}^{(+)}\langle\varphi_{\vec{p}}|. \tag{5}$$

We use standard Jacobi momenta $\vec{p}$ and $\vec{q}$ [13] to describe the motions in the two-nucleon subsystem and for the third particle in relation to the subsystem. Further H_0 is the free $3N$ Hamiltonian and V the NN potential. The nucleon mass is denoted by m.

With these definitions and using the fact that $PG_0^{-1}|\phi_{\vec{q}_0}\rangle = PV|\phi_{\vec{q}_0}\rangle$ one can transform Eq. (1) to

$$U = \mathcal{V} + \mathcal{V}G_dU, \tag{6}$$

with

$$\mathcal{V} = PV + PVG_c\mathcal{V}. \tag{7}$$

Projecting Eq. (6) onto the channel states $|\phi_{\vec{q}}\rangle$ one gets

TABLE I. The total cross section ($\sigma_{\rm tot}$) and the integrated elastic scattering angular distribution ($\sigma_{\rm el}$) obtained from the solution of the Faddeev equation (exact) and in two approximations to the effective n-d interaction ($\mathcal{V}^a, \mathcal{V}^a+\mathcal{V}^b$).

$E_{\rm lab}$(MeV)		$\sigma_{\rm tot}$(mb)	$\sigma_{\rm el}$(mb)
	exact	$0.9891E+03$	$0.8394E+03$
10	$\mathcal{V}^a$	$0.7243E+03$	$0.7247E+03$
	$\mathcal{V}^a+\mathcal{V}^b$	$0.1099E+04$	$0.9524E+03$
	exact	$0.1209E+03$	$0.5163E+02$
65	$\mathcal{V}^a$	$0.2158E+02$	$0.2159E+02$
	$\mathcal{V}^a+\mathcal{V}^b$	$0.1331E+03$	$0.6059E+02$
	exact	$0.2597E+02$	$0.5126E+01$
140	$\mathcal{V}^a$	$0.2042E+01$	$0.2043E+01$
	$\mathcal{V}^a+\mathcal{V}^b$	$0.2924E+02$	$0.5366E+01$
	exact	$0.1080E+02$	$0.1235E+01$
200	$\mathcal{V}^a$	$0.6138E+00$	$0.6139E+00$
	$\mathcal{V}^a+\mathcal{V}^b$	$0.1186E+02$	$0.1275E+01$
	exact	$0.5756E+01$	$0.6998E+00$
300	$\mathcal{V}^a$	$0.1496E+00$	$0.1496E+00$
	$\mathcal{V}^a+\mathcal{V}^b$	$0.5595E+01$	$0.7841E+00$

$$\langle\vec{q}|\langle\varphi_d|U|\varphi_d\rangle|\vec{q}\,'\rangle = \langle\vec{q}|\langle\varphi_d|\mathcal{V}|\varphi_d\rangle|\vec{q}\,'\rangle + \int d\vec{q}\,''\langle\vec{q}|\langle\varphi_d|\mathcal{V}|\varphi_d\rangle|\vec{q}\,''\rangle \times \frac{1}{E-E_d-(3/4m)q''^2+i\varepsilon}\langle\vec{q}\,''|\langle\varphi_d|U|\varphi_d\rangle|\vec{q}\,'\rangle. \quad (8)$$

This is an effective single-particle equation for the scattering of the nucleon from the deuteron. The interaction is the optical potential $\mathcal{V}(\vec{q},\vec{q}\,')$ defined by

$$\mathcal{V}(\vec{q},\vec{q}\,')\equiv\langle\vec{q}|\langle\varphi_d|\mathcal{V}|\varphi_d\rangle|\vec{q}\,'\rangle. \quad (9)$$

For a numerical realization it is convenient to introduce the operators t_c and T_c defined as

$$VG_c\equiv t_cG_0,$$
$$VG_c\mathcal{V}\equiv T_c. \quad (10)$$

Applying VG_c from the left to Eq. (7) one gets

$$T_c=t_cG_0PV+t_cG_0PT_c \quad (11)$$

and the optical potential $\mathcal{V}$ is expressed with the help of T_c by

$$\mathcal{V}=PV+PT_c. \quad (12)$$

It is easy to determine t_c. Using Eqs. (3) and (10) one gets

$$tG_0=VG=VG_d+VG_c=VG_d+t_cG_0, \quad (13)$$

which leads to

$$t_c=t-VG_dG_0^{-1}=V(1-G_0V)^{-1}-VG_dG_0^{-1}. \quad (14)$$

Finally applying $(1-G_0V)$ from the right one ends up with

$$t_c=V-V|\varphi_d\rangle\langle\varphi_d|+t_cG_0V. \quad (15)$$

The difference between t_c and t, as reflected in different leading terms of their Lippmann-Schwinger equations, exists only in the ''deuteron channel'' (the ${}^3S_1-{}^3D_1$ partial wave state). In addition, in this channel t_c is not singular, whereas t has a single pole at the deuteron binding energy.

Equations (8), (11), (12), and (15) offer a new scheme of solving the nucleon-deuteron scattering problem by first determining the optical potential and solving an effective single particle equation. Now we decompose Eq. (8) into partial waves and use our standard momentum space basis states [13]

$$|pq\alpha\rangle\equiv\left|p(ls)j\ q\left(\lambda\frac{1}{2}\right)I\ (jI)JM\ \left(t\frac{1}{2}\right)T\right\rangle, \quad (16)$$

with $(ls)j,t$ the angular momenta and isospin quantum numbers in the two-nucleon subsystem, $(\lambda\frac{1}{2})I,\frac{1}{2}$ the corresponding quantum numbers for the spectator nucleon, and J, T, and $\pi=(-1)^{l+\lambda}$ the total angular momentum, isospin, and parity of the three nucleon system. Then

$$\langle\vec{q}\,'|\langle\varphi_d|U|\varphi_d\rangle|\vec{q}\rangle = \sum_{J,\pi}\sum_{\lambda',I'}\sum_{\lambda,I} U^{J^\pi}_{\lambda'I',\lambda I}(q',q) \times\sum_{\mu'}\langle 1m_{d'}I'\mu'|Jm_{d'}+\mu'\rangle\langle\lambda'\mu'-m'\tfrac{1}{2}m'|I\mu'\rangle \times Y_{\lambda',\mu'-m'}(\hat{q}')\sum_{\mu}\langle 1m_dI\mu|Jm_d+\mu\rangle \times\langle\lambda\mu-m\tfrac{1}{2}m|I\mu\rangle Y^{\star}_{\lambda,\mu-m}(\hat{q})\,\delta_{m_{d'}+\mu',m_d+\mu}, \quad (17)$$

where

$$U^{J^\pi}_{\lambda'I',\lambda I}(q',q)\equiv\sum_{l=0,2}\sum_{l'=0,2}\int_0^\infty dp'p'^2\int_0^\infty dpp^2\varphi_{l'}(p') \times\langle p'q'\alpha_d'|U|pq\alpha_d\rangle\varphi_l(p). \quad (18)$$

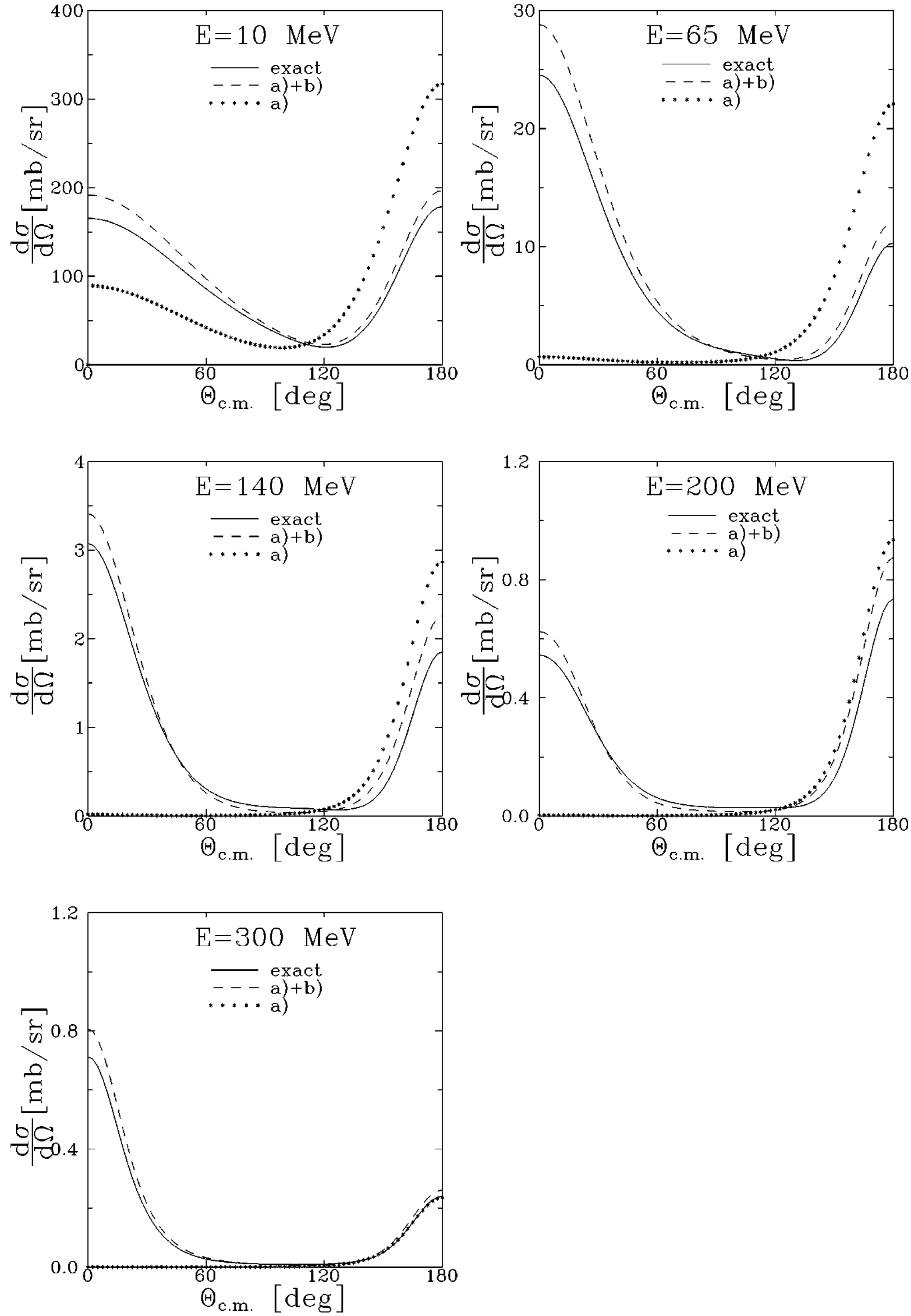

FIG. 1. The n-d elastic scattering cross section at different laboratory energies of the incoming neutron. The solid line results from the solution of the Faddeev equation. The dashed and dotted lines result in $\mathcal{V}^a$ and $\mathcal{V}^a+\mathcal{V}^b$ approximations for the effective nucleon-deuteron potential, respectively.

The two deuteron wave function components are $\varphi_l(p)$, and α_d are the three-nucleon quantum numbers with a deuteron in the two-body subsystem:

$$\{\alpha_d\}=\left\{(l=0,2;\ s=1)j=1,\left(\lambda\frac{1}{2}\right)IJ\left(0\frac{1}{2}\right)\frac{1}{2}\right\}. \tag{19}$$

The corresponding steps can be carried through for $\mathcal{V}$. Defining

$$\widetilde{U}^{J^\pi}_{\lambda' I',\lambda I}(q',q)\equiv(4m/3)U^{J^\pi}_{\lambda' I',\lambda I}(q',q),$$

$$\widetilde{\mathcal{V}}^{J^\pi}_{\lambda' I',\lambda I}(q',q)\equiv(4m/3)\mathcal{V}^{J^\pi}_{\lambda' I',\lambda I}(q',q), \tag{20}$$

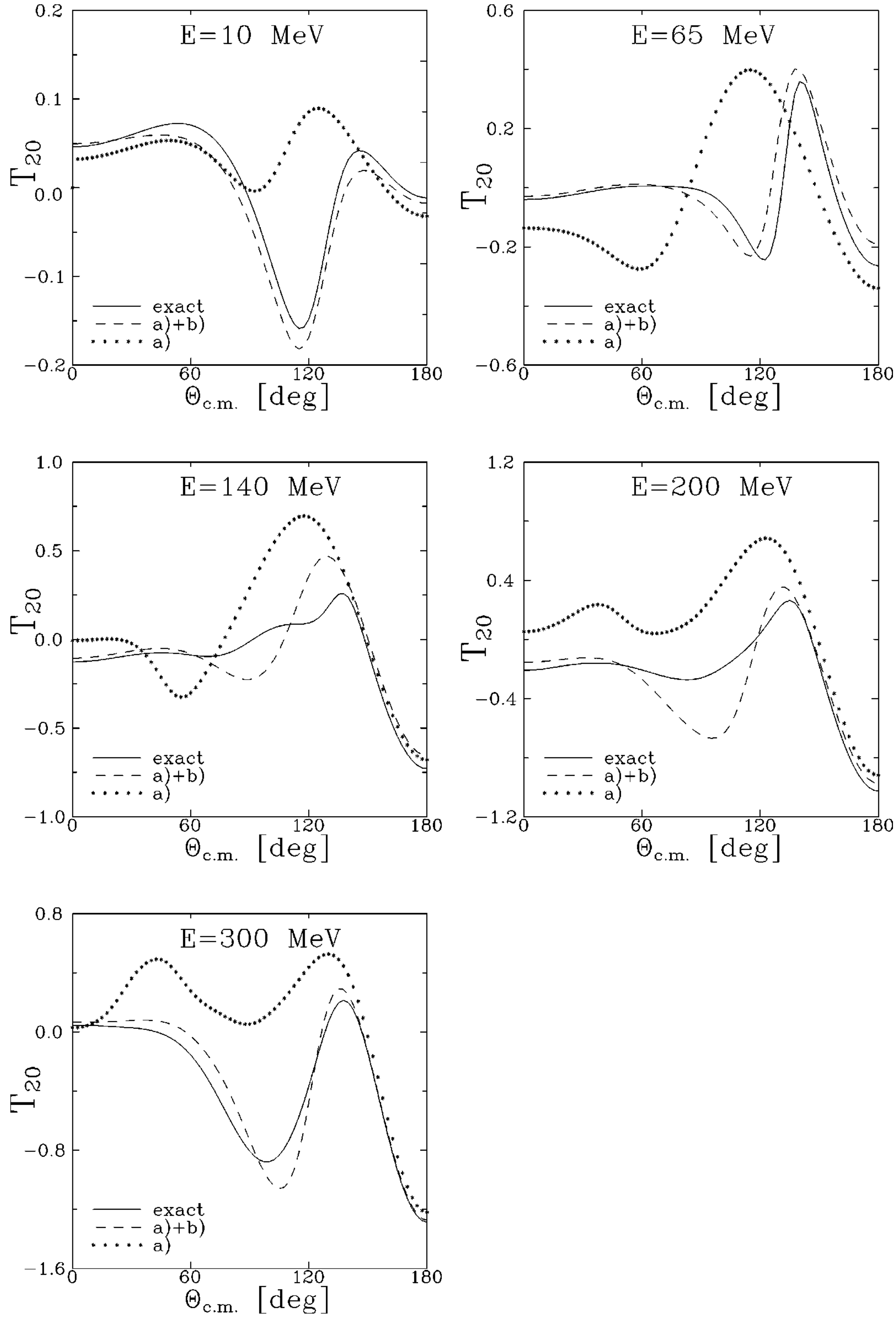

FIG. 2. The same as in Fig. 1 but for the deuteron tensor analyzing power T_{20}.

Eq. (8) achieves the form

$$\widetilde{U}^{J^{\pi}}_{\lambda' I',\lambda I}(q,q') = \widetilde{\mathcal{V}}^{J^{\pi}}_{\lambda' I',\lambda I}(q,q') + \sum_{\lambda'',I''} \int_0^{\infty} dq'' q''^2 \times \frac{\widetilde{\mathcal{V}}^{J^{\pi}}_{\lambda' I',\lambda'' I''}(q,q'')\,\widetilde{U}^{J^{\pi}}_{\lambda'' I'',\lambda I}(q'',q')}{q_0^2 - q''^2 + i\varepsilon} \tag{21}$$

with

$$E = \frac{3}{4m} q_0{}^2 - E_d . \tag{22}$$

In contrast to the described formalism our standard way to solve the n-d scattering problem is to use a Faddeev equation for the T operator defined by

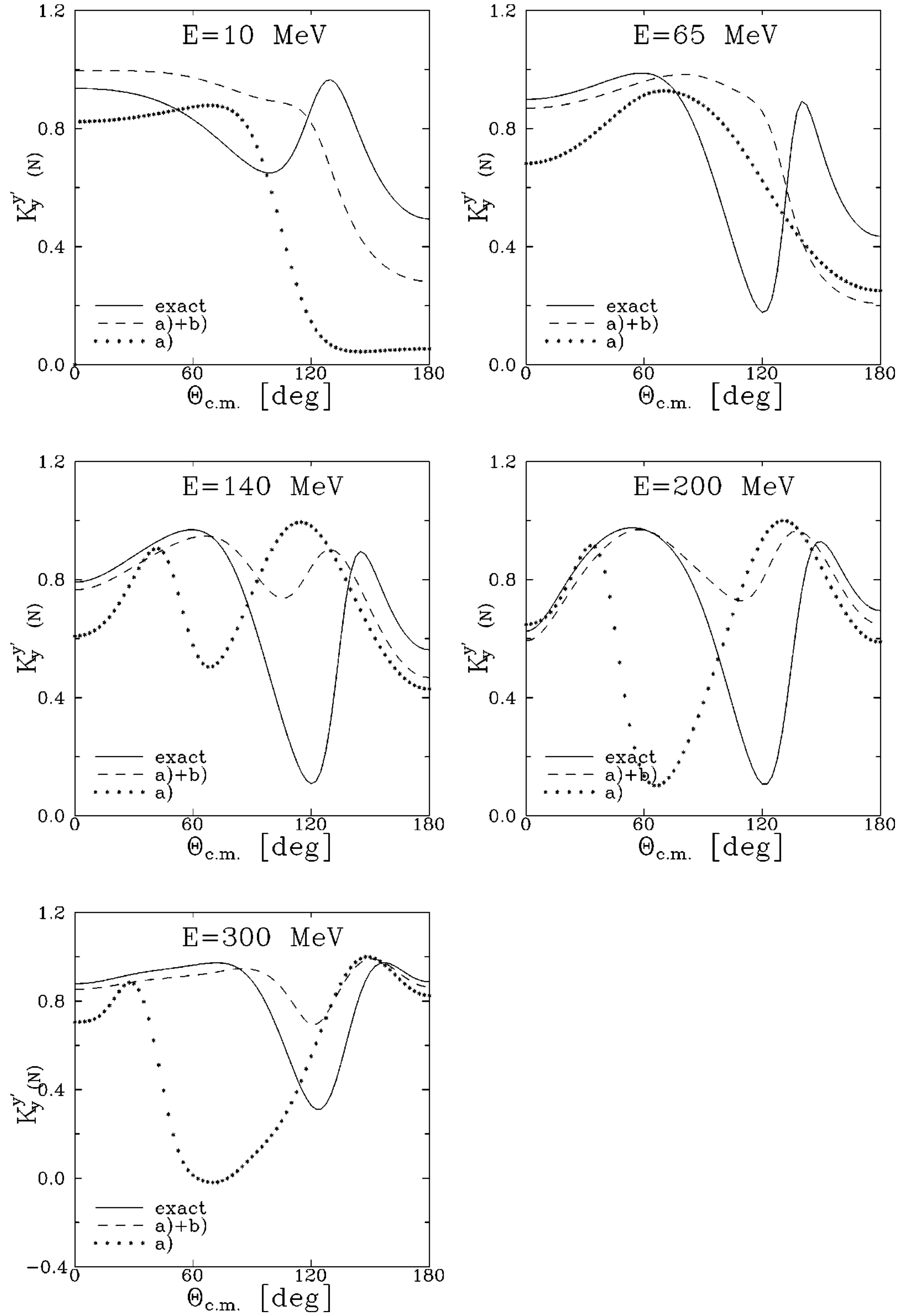

FIG. 3. The same as in Fig. 1 but for the nucleon to nucleon polarization transfer coefficient $K_y{}^{y'}$.

$$T = tG_0U. \tag{23}$$

From Eq. (1) one gets the integral equation

$$T = tP + tPG_0T, \tag{24}$$

which we solve, and U is determined via

$$U = PG_0^{-1} + PT \tag{25}$$

by quadrature.

We refer to [1–3] for the description of the method to solve numerically Eq. (24). We use the observables for elastic n-d scattering obtained from Eqs. (24) and (25) as standards to which we compare the results obtained by different approximations to the optical potential formalism.

The kernels in Eqs. (11) and (24) are very similar, only t is replaced by t_c. This suggests that the numerical technique used to solve Eq. (24) could be applied directly to Eq.

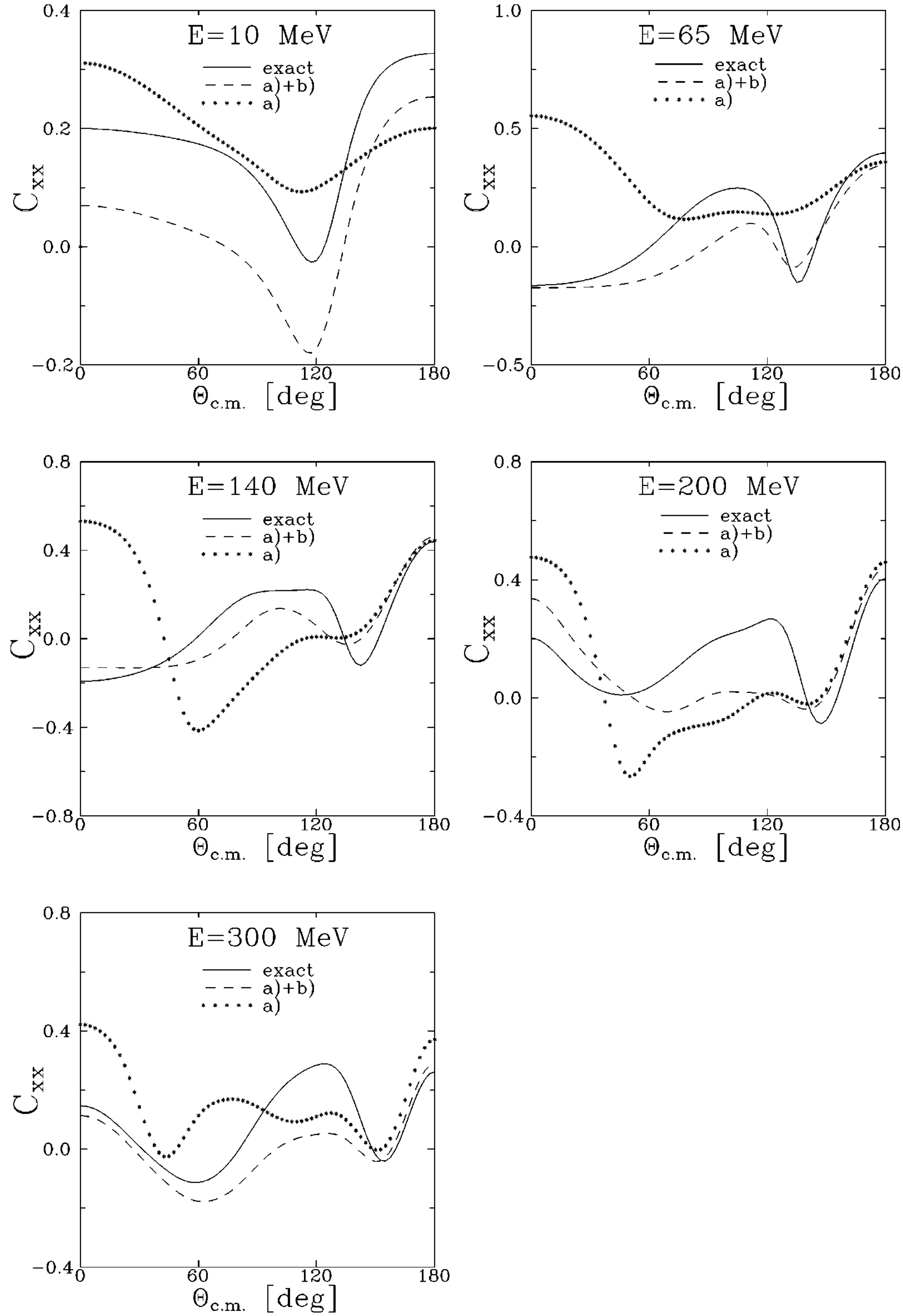

FIG. 4. The same as in Fig. 1 but for the spin correlation coefficient C_{xx}.

(11). Unfortunately the leading term $t_c G_0 P V$ in Eq. (11) has logarithmic singularities, when expressed in the basis $|pq\alpha\rangle$. As a consequence the action of the kernel in Eq. (11) on that driving term is very hard to evaluate, since G_0 in that kernel also produces logarithmic singularities. Their confluence is a quite hard technical challenge, which we did not want to tackle. In contrast in Eq. (24) the driving term is not singular and there are ''only'' the logarithmic singularities of the propagator G_0, which we can handle. Therefore we restricted ourselves to the lowest order terms for the optical potential [see Eqs. (12) and (11)]:

$$\mathcal{V} = \mathcal{V}^{a} + \mathcal{V}^{b} = PV + Pt_c G_0 PV. \tag{26}$$

The two terms partial wave projected into the deuteron channel $\mathcal{V}^{a,b}_{\lambda I,\lambda' I'}(q,q')$ are given in the Appendix.

It should be pointed out that the calculation of the second

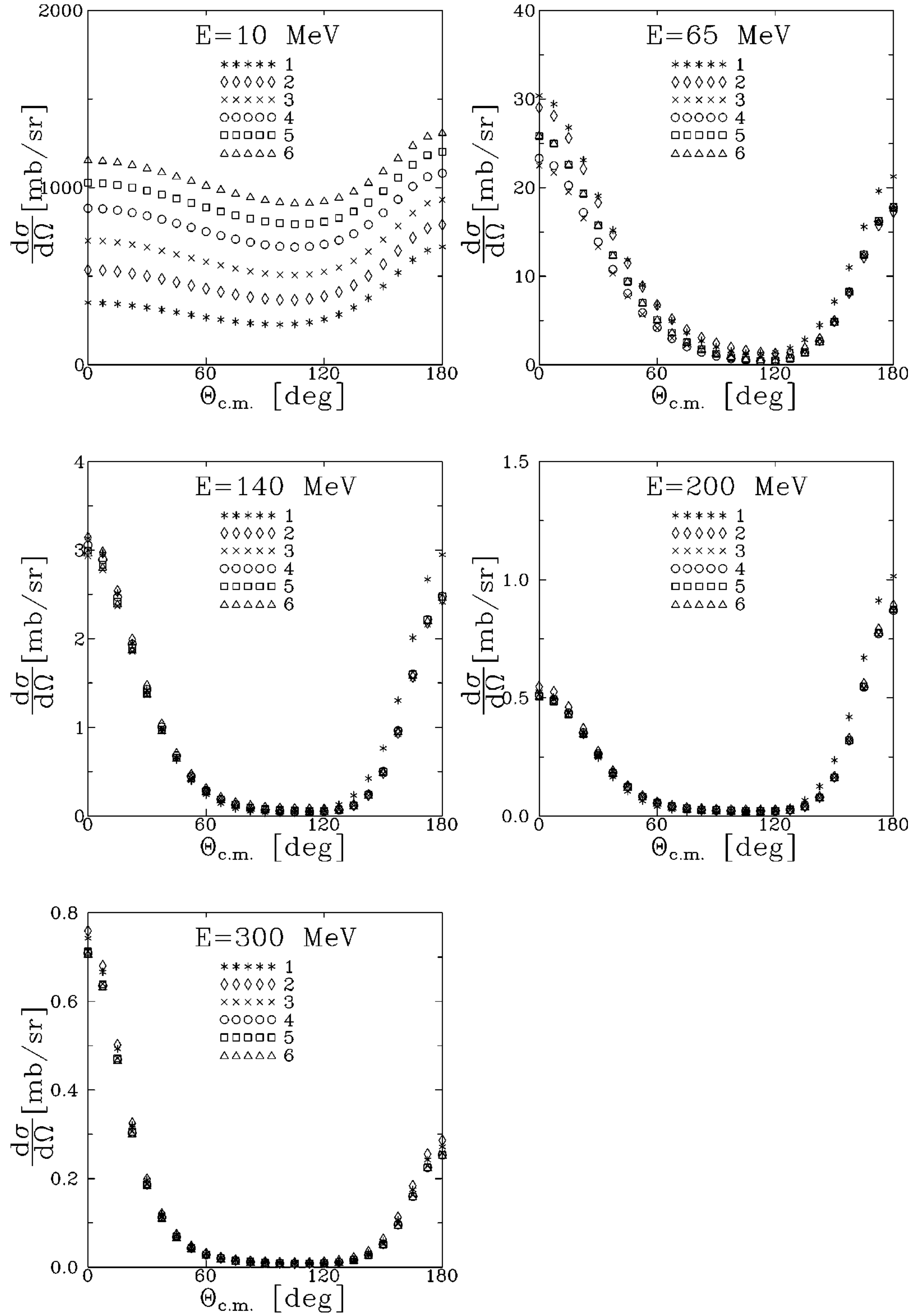

FIG. 5. The convergence properties of the leading term $\mathcal{W}$ to the transition operator U [see Eq. (29)] summed up to various orders of the continuous part t_c of the two-nucleon t matrix. Elastic scattering cross section presented by stars, rombs, crosses, circles, squares, and triangles corresponds to $\mathcal{W}$ in first, second, third, fourth, fifth, and sixth order in t_c.

term $\mathcal{V}^{b}_{\lambda' I',\lambda I}(q,q')$ is as hard a numerical problem as the exact solution of the Faddeev equations for the T operator [Eq. (24)]. One meets here the same pattern of moving singularities. Going to the next terms for $\mathcal{V}$ would require to deal with even more complicated patterns of singularities making their numerical treatment even more difficult. All this shows how difficult it is to exactly determine the optical potential for n-d scattering. According to this experience this excludes it as a practical method for solving the n-d scattering problem. It remains to be seen whether at least the low order terms are useful.

In the following we will restrict ourselves to the approximation of $\mathcal{V}$ given in Eq. (26) and study its quality at different 3N energies. The second term is of first order in t_c and

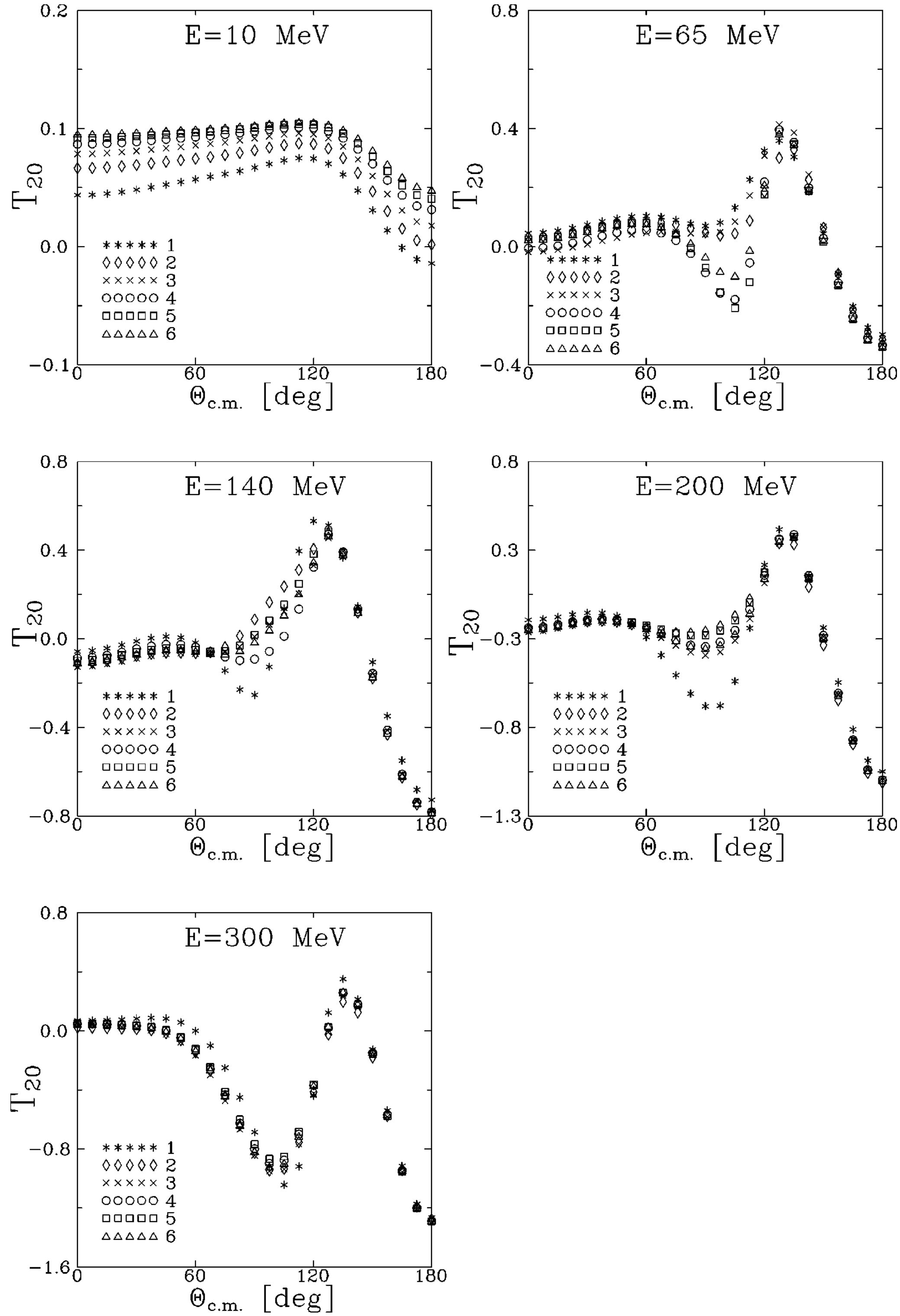

FIG. 6. The same as in Fig. 5 but for the tensor analyzing power T_{20}.

is qualitatively related to the standard expression for inter mediate energy optical potential expressions, which are also of first order in t. Our aim is to investigate, whether that truncation is sufficient in the n-d case.

III. RESULTS

We determined the approximations $\mathcal{V}^a$ and $\mathcal{V}^a+\mathcal{V}^b$ to the optical n-d potential using as the underlying NN force the Bonn B [14] potential. We restricted that force to the two strongest components acting in the $^1S_0$ and $^3S_1-{}^3D_1$ states. Therefore this is only a model study, but we do not expect a qualitative change in keeping also p-wave NN forces and higher ones. With this dynamical input we solved the Faddeev equation for the T operator at five nucleon lab energies $E^N_{\rm lab}=10$, 65, 140, 200, and 300 MeV generating ‘‘exact’’ elastic scattering observables. They form the reference val-

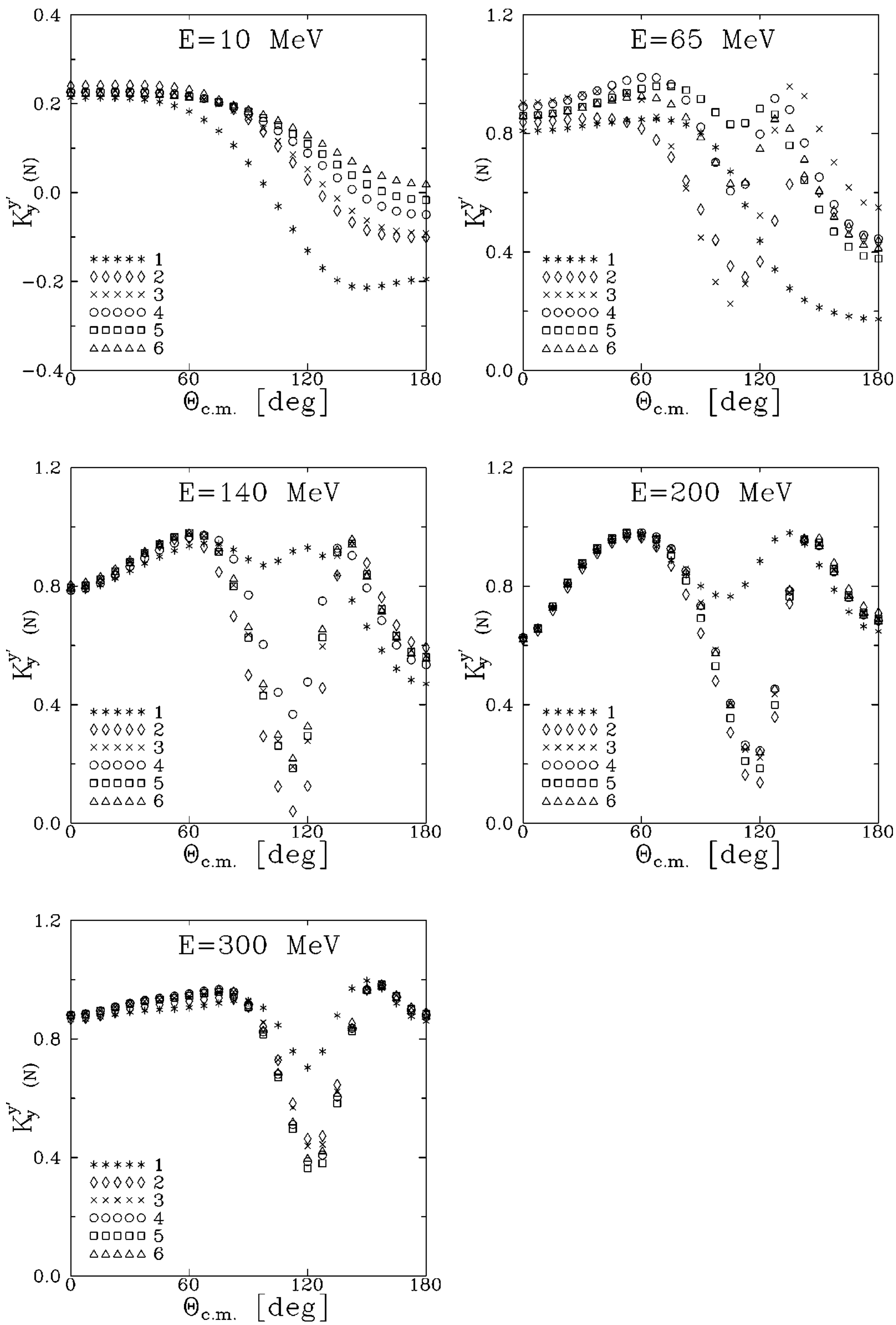

FIG. 7. The same as in Fig. 5 but for the nucleon to nucleon spin transfer coefficient $K_y^{y'}$.

ues by which we can judge the quality reached by our approximations.

In Table I we show the total cross sections evaluated through the optical theorem together with the total elastic scattering cross sections. At all energies there are clear discrepancies between the exact results and those obtained in $\mathcal{V}^a$ and $\mathcal{V}^a+\mathcal{V}^b$ approximations. Increasing the incoming nucleon energy does not diminish this disagreement sufficiently well, e.g., to a few percent. It is interesting to note that for the $\mathcal{V}^a$ approximation the total cross section and the integrated elastic scattering cross section coincide. It reflects the fact that in this approximation the effective interaction is real, which forbids the breakup processes. That $\mathcal{V}^a$ potential arises from antisymmetrization and thus dominantly governs the angular distribution at backward angles. This is apparent from Fig. 1.

In Fig. 1 the angular distribution for elastic scattering is shown. At all energies the exchange term $\mathcal{V}^a$ gives a char-

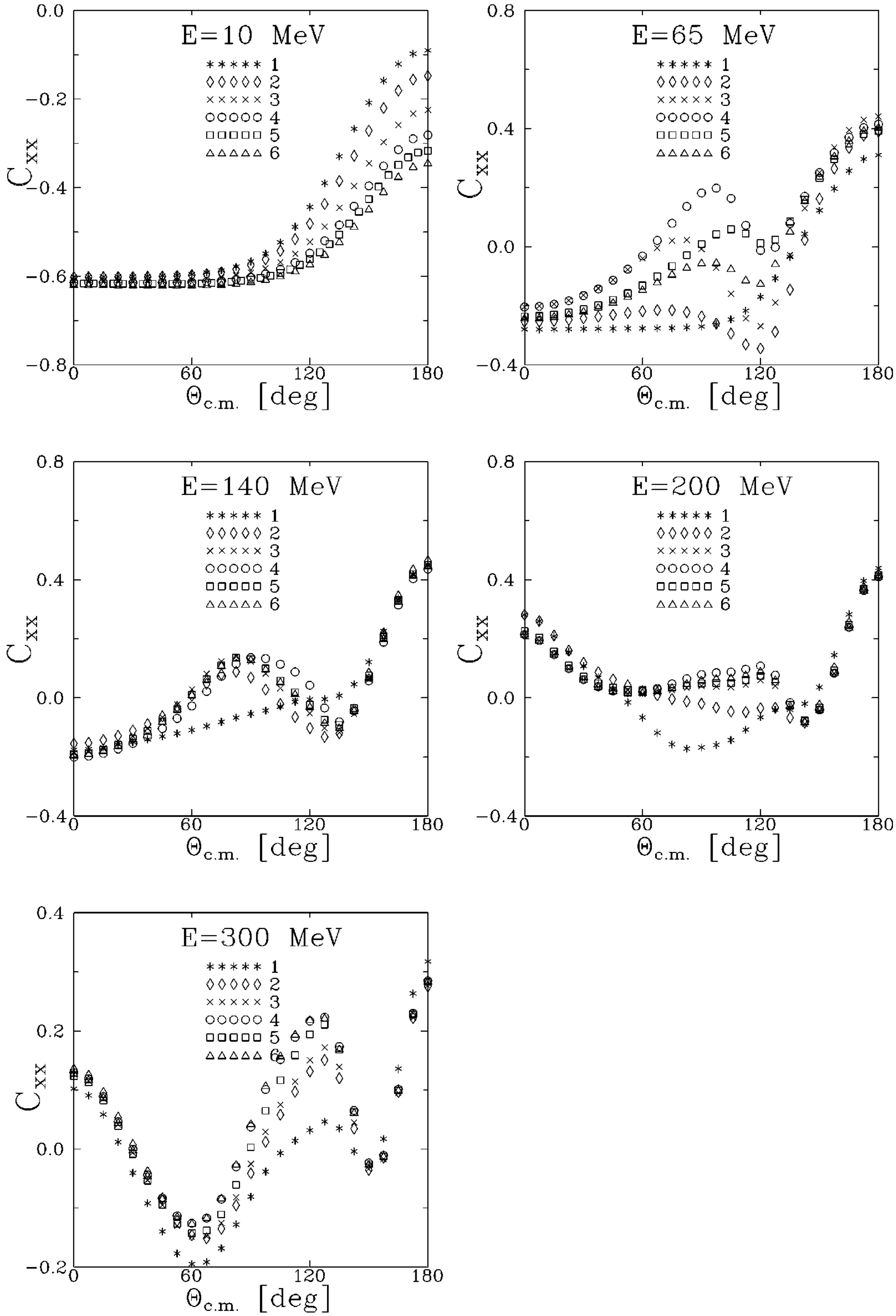

FIG. 8. The same as in Fig. 5 but for the spin correlation coefficient C_{xx}.

acteristic angular distribution, which is peaked at backward angles and which is quite different from the exact results except for the highest energy. Adding the $\mathcal{V}^b$ term brings the cross sections in the direction of the exact values. However, even at 300 MeV a clear discrepancy, especially in the forward and backward angles is left.

In Figs. 2–4 some *n-d* polarization observables are shown. The $\mathcal{V}^a+\mathcal{V}^b$ approximation disagrees with the exact results at all angles, except at forward ones where T_{20} and the spin transfer coefficient are close to the exact results.

These results clearly show that the $\mathcal{V}^a+\mathcal{V}^b$ approximation does not include sufficiently well all the details of the effective nucleon-deuteron interaction, if one wants to describe the observables at all angles. Higher order terms in t_c [Eqs. (11),(12)] would have to be added in order to get a better description for the optical potential. These rescattering processes of second order in t_c or even higher are, however, very difficult to evaluate. If, on the other hand, one focuses

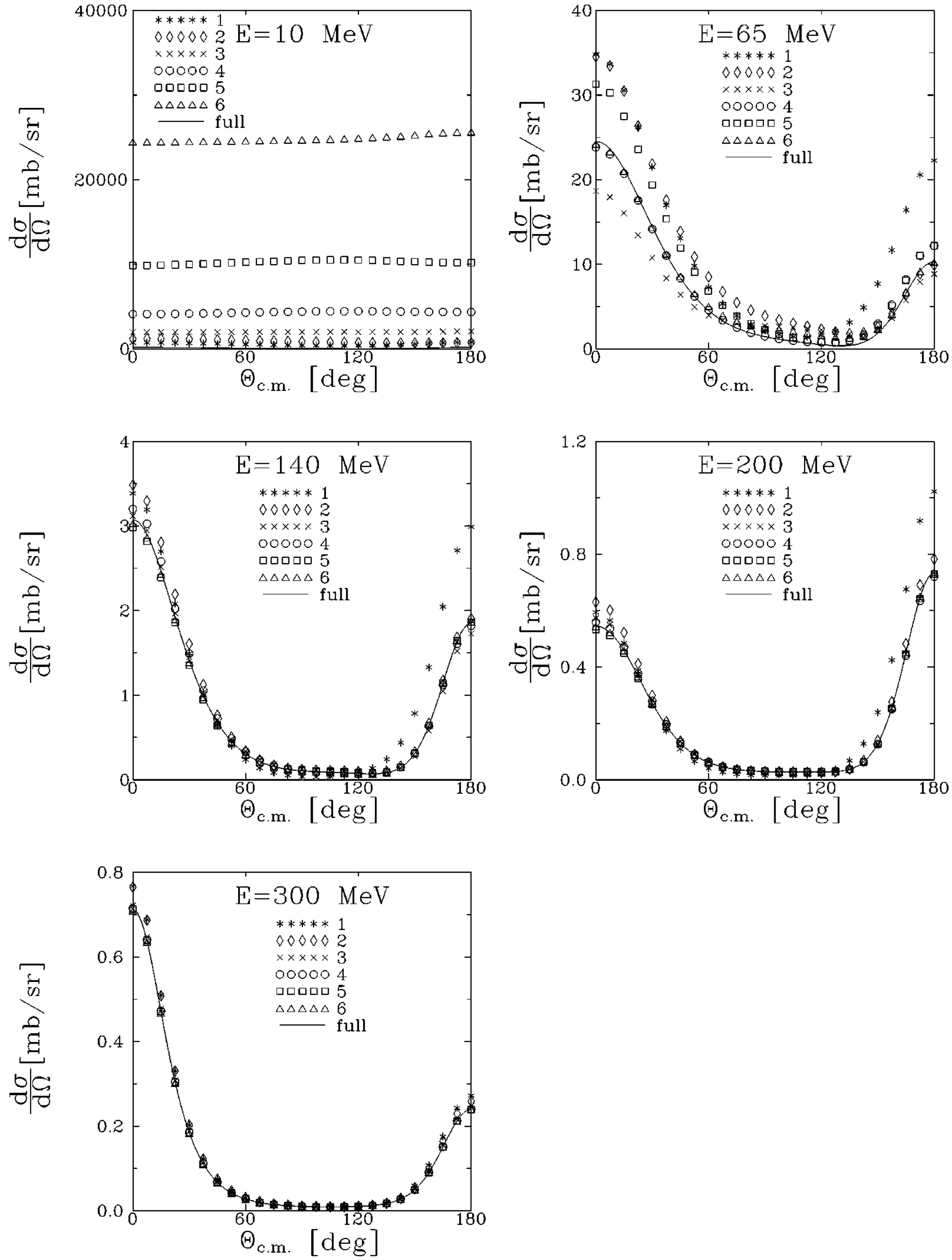

FIG. 9. The convergence properties of the n-d elastic scattering differential cross section with respect to the order of the two-nucleon t matrix t. The solid line is a fully converged exact result. Different symbols: stars, rombs, crosses, circles, squares, and triangles, are results obtained when the Neumann series for the T operator [Eq. (24)] is truncated at first, second, third, fourth, fifth, and sixth order of the t matrix, respectively.

only on the forward angles, e.g., smaller than 50°, there are spin observables which are described reasonably well by that $\mathcal{V}^{a}+\mathcal{V}^{b}$ approximation. This is also true to a smaller extent for the differential cross section.

Now there is a different form to express the optical potential, which can be used to evaluate higher order terms in a simple manner for the on-shell matrix elements. We can put Eq. (1) into the form

$$U=PG_0^{-1}+PVG_dU+PVG_cU. \tag{27}$$

Then defining

$$\mathcal{W}\equiv PG_0^{-1}+PVG_c\mathcal{W} \tag{28}$$

one gets

$$U=\mathcal{W}+\mathcal{W}G_0VG_dU. \tag{29}$$

This equation does not have the standard form where the driving term acts also as the potential in the integral kernel. But projected onto channel states it leads to a single particle

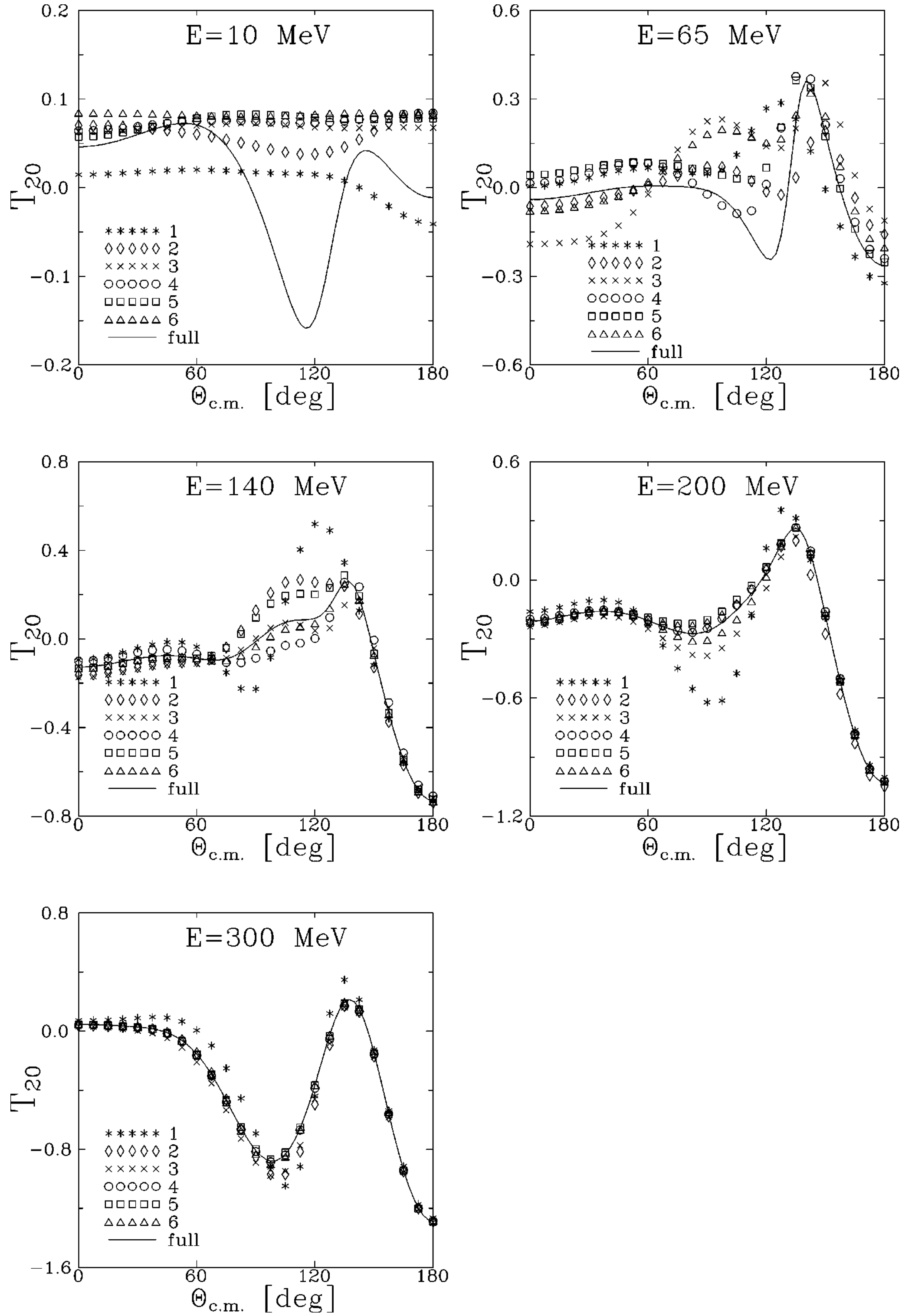

FIG. 10. The same as in Fig. 9 but for the deuteron tensor analyzing power T_{20}.

equation for the elastic *n*-*d* scattering amplitude similar to Eq. (8). The connection of $\mathcal{W}$ to $\mathcal{V}$ is simply

$$\mathcal{W} G_0 V = \mathcal{V} \tag{30}$$

and U from Eq. (29) provides the same on-shell matrix elements as U from Eq. (8) since $G_0 V \phi^-_{\vec{q}_0} = \phi^-_{\vec{q}_0}$. That $\mathcal{W}$ operator is directly expressed as a multiple scattering series in t_c as easily follows from Eq. (28):

$$\mathcal{W} = P G_0^{-1} + P t_c P + P t_c G_0 P t_c P + \cdots . \tag{31}$$

That series can be evaluated through an integral equation defining

$$\mathcal{W} = P G_0^{-1} + P \widetilde{T}_c , \tag{32}$$

where $\widetilde{T}_c$ obeys

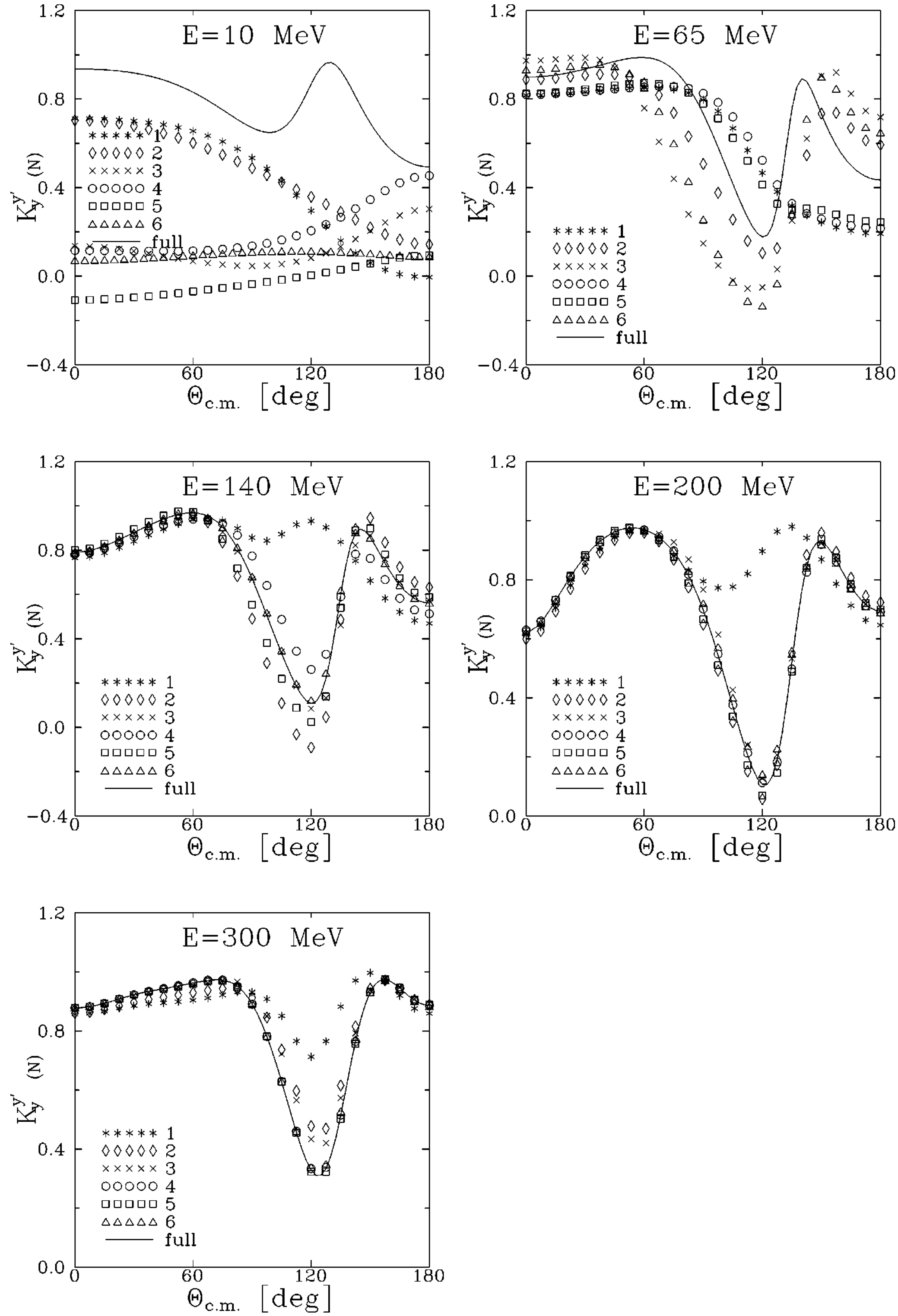

FIG. 11. The same as in Fig. 9 but for the nucleon to nucleon spin transfer coefficient $K_y^{y'}$.

$$\widetilde{T}_c = t_c P + t_c G_0 P \widetilde{T}_c. \tag{33}$$

The advantage of the form Eq. (29) is now that at least the on-shell matrix elements of $\mathcal{W}$ can be evaluated to arbitrary order in t_c. Clearly if that multiple scattering series requires higher order terms, then due to Eq. (30) also the previous form of the optical potential will require them. For the evaluation of the $\mathcal{W}$ operator in the kernel of Eq. (29) again the same remarks apply as for $\mathcal{V}$ in Sec. II. That $\mathcal{W}$ evaluated through Eqs. (32) and (33) will suffer from logarithmic singularities already in the driving term and the iteration of that object causes very tough numerical obstacles.

Thus we restricted ourselves to the Born approximation for Eq. (29) and evaluated the multiple scattering series for

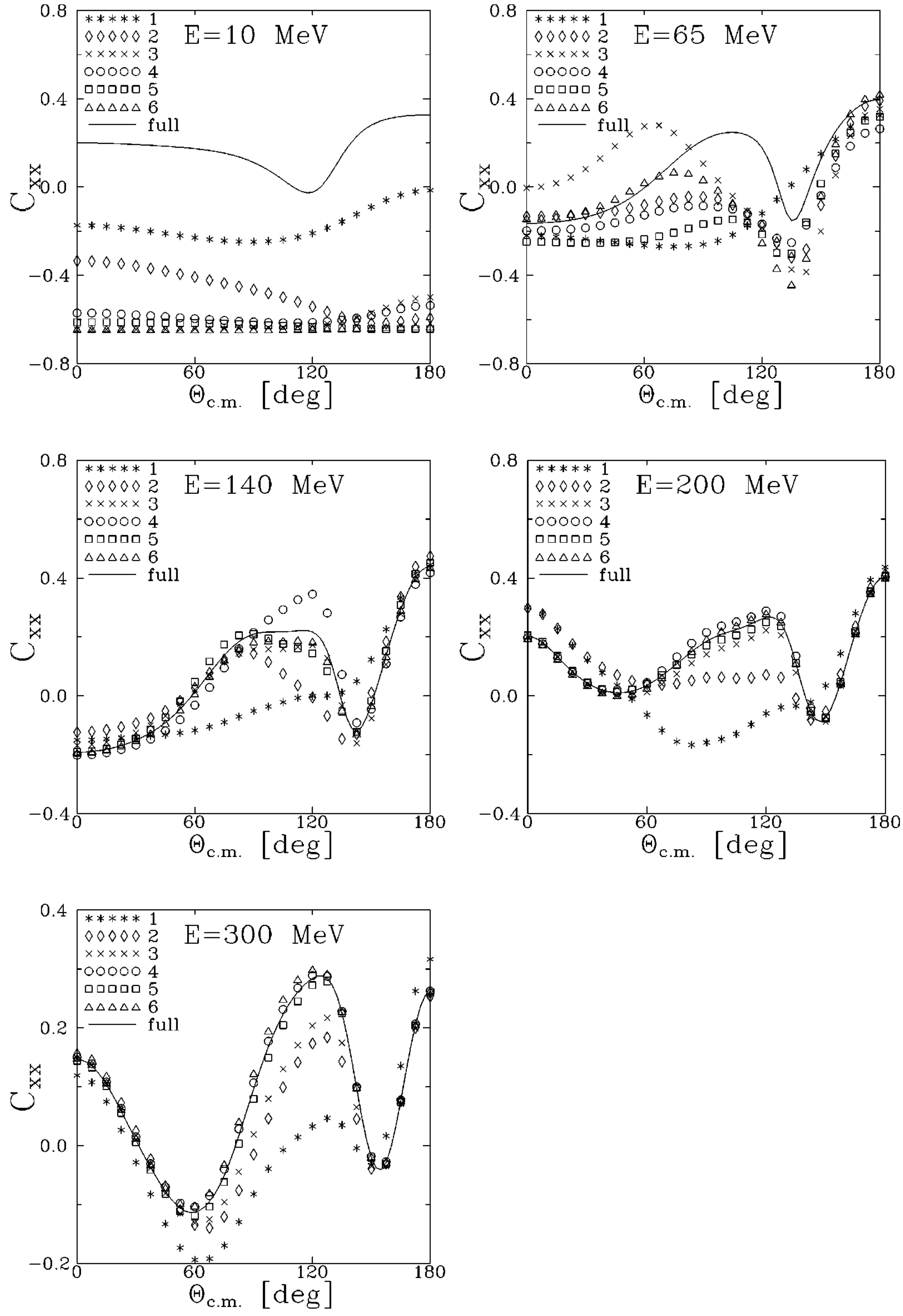

FIG. 12. The same as in Fig. 9 but for the spin correlation coefficient C_{xx}.

$\widetilde{T}_c$ via Eq. (33) applied only to the on-shell channel state. This generated via Eq. (32) elastic scattering amplitudes in various orders in t_c. The resulting elastic scattering observ ables partially summed up to certain orders in t_c are shown in Figs. 5–8. It is clearly seen that there is no convergence with respect to t_c at our lowest energy of 10 MeV. At higher energies the cross sections series starts to converge and the third order is sufficient. However, no convergence is indicated, even at high energies, for spin observables with exception of the forward angular region. Therefore, if one focuses again only on forward angles, convergence is found and low orders are sufficient.

We have to conclude that the optical n-d potential for the energies considered cannot be truncated at the first order term in t_c if one wants to describe observables at all angles. At small c.m. angles, however, low order truncations are quite acceptable. This is the angular region, which is mostly studied in nucleon-nucleus scattering for heavier-targets, since the cross section drops quickly by several orders of magnitude from 0° to about 60°. And for that restricted angular region the lowest order truncation appears to be successful for heavier systems [15–17]. Our results can therefore be considered to support that.

In view of our results an interesting question arises: how important are the rescattering effects of orders higher than 1 in the nucleon-nucleon t matrix for elastic neutron-deuteron scattering? To that aim we regard the multiple scattering series in the full NN t operator t for the operator U of elastic scattering. That series is defined through Eqs. (24) and (25) and reads

$$U = PG_0^{-1} + PtP + PtPG_0tP + \cdots. \tag{34}$$

The predictions summed up to different order in t for some scattering observables are compared to the exact results in Figs. 9–12. At the lowest energy of 10 MeV there is no convergence in that series in the t matrix for any of the elastic scattering observables. That strong divergence is caused by the $J^{\pi}=\frac{1}{2}^{+}$ contribution, which is the quantum number of the 3N bound state and whose existence is responsible for that divergence. At higher energies the contribution of $J^{\pi}=\frac{1}{2}^{+}$ diminishes and a tendency for convergence appears. However, even at 300 MeV the sixth order rescattering is needed for some observables to reproduce the exact results. Even more, at 200 and 300 MeV the first order term in t is not acceptable, except at forward angles, and C_{xx} excluded.

These results are presumably not surprising since the series Eq. (34) includes the intermediate propagation in the deuteron channel and thus the iteration of the optical potential, which is not small. But even rewriting the series Eq. (34) into the optical potential form, we found that the multiple scattering series for the optical potential, now in the truncated t_c operator, does not converge fast enough to justify in general a first order approximation in t_c.

IV. CONCLUSIONS

Starting from the AGS equations we developed an equivalent formulation of the 3N scattering introducing an effective nucleon-deuteron interaction, usually called an optical potential. The resulting integral equation for this interaction contains all the hard tasks of the 3N problem with its complicated pattern of singularities. Thus, in spite of the simplicity of the n-d system, the determination of that effective interaction is a hard numerical task. In a model study we restricted the NN force to the $^1S_0$ and $^3S_1-{}^3D_1$ channels. Further we restricted ourselves to the exchange term and the term linear in the continuum part of the two-nucleon t matrix. Such an approximation is, however, not sufficient even at as high energies as 300 MeV to describe the observables at all angles. Further, our study of the convergence properties of the transition operator for the n-d elastic scattering operator U reveals that the restriction to the first leading terms in the two-nucleon t matrix is not sufficient. However if one focuses on forward angles only, lower orders in the NN t matrix turn into a reasonable approximation, depending on the energy and observables. This latter point supports the validity of first order optical potential studies at higher energies for forward angles, where they are successfully applied.

ACKNOWLEDGMENTS

We would like to thank Charlotte Elster for very constructive criticisms. This work was supported by the Deutsche Forschungsgemeinschaft (H.W.) and by the Polish Committee for Scientific Research under Grant No. 2 P302 104 06. The numerical calculations were performed on the Cray T90 of the Höchstleistungsrechenzentrum in Jülich, Germany, and on the Convex 3820 of the Academic Computational Center (ACK) in Cracow, Poland.

APPENDIX

Performing the projection of PV onto the $|pq\alpha\rangle$ basis states and using the corresponding matrix elements for the permutation operator P [13] one gets

$$\begin{aligned}\langle pq\alpha|PV|p'q'\alpha'\rangle &= \sum_{l_{\overline{\alpha'}}}\int_0^{\infty} dp'' p''^2 \langle pq\alpha|P|p''q'\overline{\alpha'}\rangle\langle p'' l_{\overline{\alpha'}}|V|p' l_{\alpha'}\rangle\\ &= \sum_{l_{\overline{\alpha'}}}\int_0^{\infty} dp'' p''^2 \int_{-1}^{1} dx \frac{\delta(p-\pi_1)}{p^{l_\alpha+2}}\,\frac{\delta(p''-\pi_2)}{p''^{l_{\overline{\alpha'}}+2}} G_{\alpha\overline{\alpha'}}(qq'x)\langle p'' l_{\overline{\alpha'}}|V|p' l_{\alpha'}\rangle\\ &= \sum_{l_{\overline{\alpha'}}}\int_{-1}^{1} dx \frac{\delta(p-\pi_1)}{p^{l_\alpha+2}} G_{\alpha\overline{\alpha'}}(qq'x)\frac{\langle \pi_2 l_{\overline{\alpha'}}|V|p' l_{\alpha'}\rangle}{\pi_2^{l_{\overline{\alpha'}}}},\end{aligned} \tag{A1}$$

where the quantum numbers in $\overline{\alpha'}$ are the same as in α with the exception of $l_{\overline{\alpha'}}$ in case of coupled two-nucleon states. In this case $l_{\overline{\alpha'}}=l_{\alpha\pm 2}$.

This leads to

$$\mathcal{V}^{a}_{\lambda I,\lambda' I'}(q,q') \equiv \sum_{l_\alpha} \sum_{l_{\alpha'}} \int_0^\infty dp' p'^2 \int_0^\infty dp p^2 \varphi_{l_\alpha}(p) \langle pq\alpha | PV | p'q'\alpha' \rangle \varphi_{l_{\alpha'}}(p')$$

$$= \sum_{l_\alpha} \sum_{l_{\alpha'}} \int_0^\infty dp' p'^2 \sum_{l_{\overline{\alpha'}}} \int_{-1}^{1} dx \frac{\varphi_{l_\alpha}(\pi_1)}{\pi_1^{l_\alpha}} G_{\alpha\overline{\alpha'}}(qq'x) \frac{\langle \pi_2 l_{\overline{\alpha'}} | V | p' l_{\alpha'} \rangle}{\pi_2^{l_{\overline{\alpha'}}}} \varphi_{l_{\alpha'}}(p'), \tag{A2}$$

with

$$\pi_1 = \sqrt{q'^2 + \tfrac{1}{4} q^2 + qq'x},$$

$$\pi_2 = \sqrt{q^2 + \tfrac{1}{4} q'^2 + qq'x}. \tag{A3}$$

In a similar way one gets

$$\mathcal{V}^{b}_{\lambda I,\lambda' I'}(q,q') \equiv \sum_{l_\alpha} \sum_{l_{\alpha'}} \sum_{\tilde{\alpha}} \int_{-1}^{1} dx \int_0^\infty dp' p'^2 \int_0^\infty d\tilde{q} \tilde{q}^2 \frac{\varphi_{l_\alpha}(\pi_1)}{\pi_1^{l_\alpha}} G_{\alpha\tilde{\alpha}}(q\tilde{q}x)$$

$$\times \int_{-1}^{1} dx' \sum_{l_{\overline{\alpha'}}} \sum_{l_{\overline{\tilde{\alpha}}}} \frac{\langle \pi_2 l_{\tilde{\alpha}} | t_c(E - (3/4m)\tilde{q}^2) | l_{\overline{\tilde{\alpha}}} \pi'_1 \rangle}{\pi'^{\,l_{\overline{\tilde{\alpha}}}}_1 \pi_2^{l_{\tilde{\alpha}}}} G_{\overline{\tilde{\alpha}}\overline{\alpha'}}(\tilde{q}q'x')$$

$$\times \frac{1}{E - 1/m(\tilde{q}^2 + q'^2 + \tilde{q}q'x') + i\varepsilon} \frac{\langle \pi'_2 l_{\overline{\alpha'}} | V | p' l_{\alpha'} \rangle}{\pi_2'^{\,l_{\overline{\alpha'}}}} \varphi_{l_{\alpha'}}(p'), \tag{A4}$$

with

$$\pi'_1 = \sqrt{q'^2 + \tfrac{1}{4} \tilde{q}^2 + \tilde{q}q'x},$$

$$\pi'_2 = \sqrt{\tilde{q}^2 + \tfrac{1}{4} q'^2 + \tilde{q}q'x}. \tag{A5}$$

[1] H. Witała, Th. Cornelius, and W. Glöckle, Few-Body Syst. **3**, 123 (1988).

[2] D. Hüber, H. Witała, and W. Glöckle, Few-Body Syst. **14**, 171 (1993).

[3] W. Glöckle, H. Witała, D. Hüber, H. Kamada, and J. Golak, Phys. Rep. **274**, 107 (1996).

[4] D. Hüber, H. Witała, A. Nogga, W. Glöckle, and H. Kamada, Few-Body Syst. (to published).

[5] K. M. Watson, Phys. Rev. **89**, 575 (1953); N. C. Francis and K. M. Watson, *ibid.* **92**, 291 (1953).

[6] A. Kerman, M. McManus, and R. M. Thaler, Ann. Phys. (N.Y.) **8**, 551 (1959).

[7] E. R. Siciliano and R. M. Thaler, Phys. Rev. C **16**, 1322 (1977); D. J. Ernst, J. T. Londergan, G. A. Miller, and R. M. Thaler, *ibid.* **16**, 537 (1977).

[8] P. C. Tandy, E. F. Redish, and D. Bolle, Phys. Rev. C **16**, 1924 (1977).

[9] C. R. Chinn, Ch. Elster, R. M. Thaler, and S. P. Weppner, Phys. Rev. C **52**, 1992 (1995).

[10] C. Mahaux, K. T. R. Davies, and G. R. Satchler, Phys. Rep. **224**, 237 (1993).

[11] Ch. Elster and W. Glöckle, Phys. Rev. C **55**, 1058 (1997).

[12] E. O. Alt, P. Grassberger, and W. Sandhas, Nucl. Phys. **B2**, 167 (1967).

[13] W. Glöckle, *The Quantum-Mechanical Few-Body Problem* (Springer-Verlag, Berlin, 1983).

[14] R. Machleidt, Adv. Nucl. Phys. **19**, 189 (1989).

[15] R. Crespo, R. C. Johnson, and J. A. Tostevin, Phys. Rev. C **41**, 2257 (1990).

[16] H. F. Arellano, F. A. Brieva, and W. G. Love, Phys. Rev. C **41**, 2188 (1990); H. F. Arellano, R. A. Brieva, and W. G. Love, *ibid.* **52**, 301 (1995); H. F. Arellano, F. A. Brieva, M. Sander, and H. V. von Geramb, Phys. Rev. C **54**, 2570 (1996).

[17] T. Cheon, Ch. Elster, E. F. Redish, and P. C. Tandy, Phys. Rev. C **41**, 841 (1990); Ch. Elster, S. P. Weppner, and C. R. Chinn (unpublished).